Saudi Journal of Biological Sciences (2017) **24**, 1243–1248

King Saud University

Saudi Journal of Biological Sciences

www.ksu.edu.sa
www.sciencedirect.com

ORIGINAL ARTICLE

Characterization and anti-*Aspergillus flavus* impact of nanoparticles synthesized by *Penicillium citrinum*

Mohamed A. Yassin [a,b,*], Abd El-Rahim M.A. El-Samawaty [a,b], Turki M. Dawoud [a], Omar H. Abd-Elkader [c,d], Khalid S. Al Maary [a], Ashraf A. Hatamleh [a], Abdallah M. Elgorban [a,b]

[a] *Botany and Microbiology Department, Faculty of Science, King Saud University, Riyadh, Saudi Arabia*
[b] *Agricultural Research Center, Plant Pathology Research Institute, Giza, Egypt*
[c] *Electron Microscope Unit, Zoology Department, College of Science, King Saud University, Saudi Arabia*
[d] *Electron Microscope & Thin Films Department, Physics Division, National Research Center, Cairo, Egypt*

Received 3 May 2016; revised 5 September 2016; accepted 3 October 2016
Available online 31 October 2016

KEYWORDS

Nanotechnology;
Seed borne;
Antimicrobial agents;
Aflatoxins

Abstract This work was conducted to evaluate the ability of grape molding fungus; *Penicillium citrinum* to synthesize silver nanoparticles (Ag NPs). The potency of biosynthesized Ag NPs was checked against the aflatoxigenic *Aspergillus flavus var. columnaris*, isolated from sorghum grains. Biosynthesized Ag NPs were characterized and confirmed in different ways. X ray diffraction (XRD), Energy Dispersive Spectroscopy (EDS), Transmission Electron Microscopy (TEM) and optical absorption measurements confirmed the bio-synthesis of Ag NPs. The *in vitro* antifungal investigation showed that biosynthesized Ag NPs were capable of inhibiting the growth of aflatoxigenic *A. flavus var. columnaris*. Utilization of plant pathogenic fungi in the Ag NPs biosynthesis as well as the use of bio-Ag NPs to control fungal plant diseases instead of chemicals is promising. Further work is needed to confirm the efficacy of the bio-Ag NPs against different mycotoxigenic fungi and to determine the potent applicable doses.

1. Introduction

Nowadays; one of the most active areas of research in the field of nanotechnology is the biosynthesis of nanoparticles with 1–100 nm size (Saxena et al., 2014). Ag NPs for example, could be synthesized using biological means instead of physical and chemical approaches (Ghorbani et al., 2011). Due to their applications in a number of areas such as agricultural production, food industries, human health and others, Ag NPs are finding more attention (Thul et al., 2013). Biosynthesis of Ag NPs using microorganisms is cost-effective, eco-friendly, easy and fast

* Corresponding author at: Botany and Microbiology Department, Faculty of Science, King Saud University, Riyadh, Saudi Arabia.
E-mail address: myassin@ksu.edu.sa (M.A. Yassin).
Peer review under responsibility of King Saud University.

Production and hosting by Elsevier

http://dx.doi.org/10.1016/j.sjbs.2016.10.004
1319-562X

compared with physical and chemical methods. A number of microorganisms such as bacteria, fungi, yeasts, and algae have been known to synthesize Ag NPs (Saxena et al., 2014).

Fungi are among the most eco-friendly nanoparticle synthesizers; hence, they are used in Ag NPs bio-synthesis. Several species of *Alternaria* (Gajbhiye et al., 2009), *Aspergillus* (Khalil, 2013), *Fusarium* (Ingle et al., 2009), *Penicillium* spp. (Singh et al., 2014), *Phoma* (Gade et al., 2014), and *Trichoderma* (Devi et al., 2013) have been reported to synthesize Ag NPs.

The success of bio-synthesized Ag NPs in controlling phytopathogenic fungi; particularly aflatoxigenic fungi; is promising in eradication or at least minimizing the mycotoxin hazards (Abdel-Hadi et al., 2014; Elgorban et al., 2015). The aflatoxigenic seed born fungus; *Aspergillus flavus var. columnaris* is dominantly isolated from sorghum grains (Yassin et al., 2013). The use of such contaminated grains could subsequently harm the human and livestock (Arapcheska et al., 2015). The current work aimed to study the bio-synthesis of silver nanoparticles using grape molding *Penicillium citrinum*. However, the antifungal activity of the obtained Ag NPs was also checked against the aflatoxigenic, seed born fungus *A. flavus var. columnaris*.

2. Materials and methods

2.1. Biomass preparation

Penicillium citrinum used in this study has originally been isolated from grapes. Fungus was grown in 250 ml Erlenmeyer flasks each containing 100 ml liquid medium containing (g/L): KH_2PO_4 7.0 g; K_2HPO_4 2.0 g; $MgSO_47H_2O$ 0.1 g; $(NH_4)_2SO_4$ 1.0 g; yeast extract 1.0 g and glucose 15.0 g. Inoculated media were incubated at 28 ± 2 °C and 180 rpm for 5 days, after which fungal biomass was separated using Whatman filter paper No. 1 and extensively washed by deionized water. The collected fungal biomass was transferred to 100 ml of deionized water in the 250 Erlenmeyer flask and further incubated at 140 rpm for 72 h in an orbital shaker. Fungal biomass was filtered again with Whatman filter paper No. 2 and the collected cell-free filtrate was subjected to biosynthesis of silver nanoparticles (Naveen et al., 2010).

2.2. Ag NPs biosynthesis

An aqueous, 1.0 mM silver nitrate solution was prepared, added to the cell-free supernatant (1:1) in the reaction flask and incubated in the dark at 28 ± 2 °C in the rotary shaker (200 rpm). Cell-free filtrate (without silver nitrate) and silver nitrate solution (without cell-free filtrate) were used as negative and positive controls. All treatments were triplicated and incubated as mentioned above until the color change into yellowish was observed (Naveen et al., 2010). Color change indicates the formation of silver nanoparticles, which were purified by centrifugation (UNIVERSAL 320/320 Rat) at 9000 rpm for 14 min. The supernatant was separated and the pellet was dried at 60 °C for 24 h in the oven.

2.3. Ag NPs characterization

The Ag NPs synthesized from *P. citrinum* were characterized and confirmed in different ways. The dried pellet was initially used in the X-ray diffraction (XRD) and Energy Dispersive Spectroscopy (EDS). However, Ag NPs solution was used for transmission electron microscope (TEM) and optical absorption measurement.

The metallic nature of biosynthesized Ag NPs was analyzed using XRD (Prema, 2010). An X Pert Pro diffractometer used Cu-Kα radiation at 40 KeV and 40 mA was used. However, scans were typically performed over a 2θ range from 10° to 85° at a speed of 0.02/s, with an aperture slit, an anti-scatter slit, and a receiving slit of 2 mm, 6 mm, and 0.2 mm, respectively. X-rays Cu-Kα wavelength was (1.54056 Å). The Ag NP structure was calculated with the help of the Full-prof and Chekcell programs (Carvajal, 1993). The EDS combined with scanning electron microscope (SEM) was then used to quantify the compositional analysis of nanoparticles. SEM (EDS, JEOL model JSM–6380) was also used to examine surface morphology of the nanoparticles.

Ag NPs solution was sonicated for 1 h using 740 and 740X Ultrasounds Sonicator prior to optical absorption measurement using UV–Vis; Shimadzu 3101 PC spectrophotometer. The investigated wave-length range was 300–900 nm, and the incident photon flux was normal to the surface. The formation of Ag NPs was finally confirmed using JEOL1010 TEM. A few drops of Ag nanoparticle solution were dropped onto a carbon coated copper grid, and the residue was removed by a filter paper beneath.

2.4. Ag NPs antifungal test

Inhibitory effects of biosynthesized Ag NPs were tested *in vitro* against *A. flavus var. columnaris*. Tested isolate used in this experiment is aflatoxigenic and mainly isolated from sorghum grains (Yassin et al., 2013). Crude silver nanoparticles were incorporated into PDA medium to obtain 50, 100, 150 and 200 ppm concentrations. Treated media were immediately poured into sterilized 90 mm Petri dishes and inoculated with 4 mm fungal plugs after quiet solidification. Triplicated treatments of Petri plates were then incubated along with the controls at 28 ± 2 °C for 10 days. The colony diameter was measured daily and % growth inhibition was calculated compared with the control.

3. Results and discussion

3.1. Ag NPs biosynthesis

Fig. 1 shows the change of the solution color into yellowish after 2 days of incubation due to the reaction of silver nitrate with the culture supernatant. The color change indicates the production of Ag NPs (Sadowski et al., 2008). However, no color change was observed in the control. Fungal extracellular enzymes are reported to play a critical role in the reduction of silver ions into Ag NPs. Gradual changes into the yellowish color generally indicate the presence of nitrate reductase enzyme that regulate Ag NPs biosynthesis (Naveen et al., 2010).

3.2. Ag NPs characterization

3.2.1. XRD analysis

Fig. 2 illustrates the XRD of biosynthesized Ag NPs. The Ag NPs are clearly polycrystalline and no crystallographic impurities spurious diffraction was observed. All the reflections

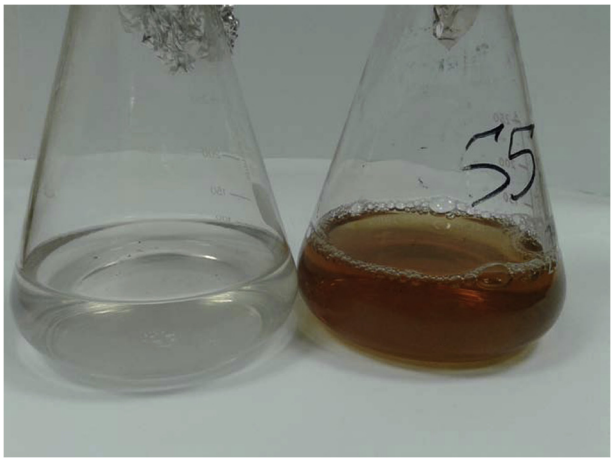

Figure 1 The reaction solution shows the color change in the culture filtrate with silver ions (b) compared with the control (a).

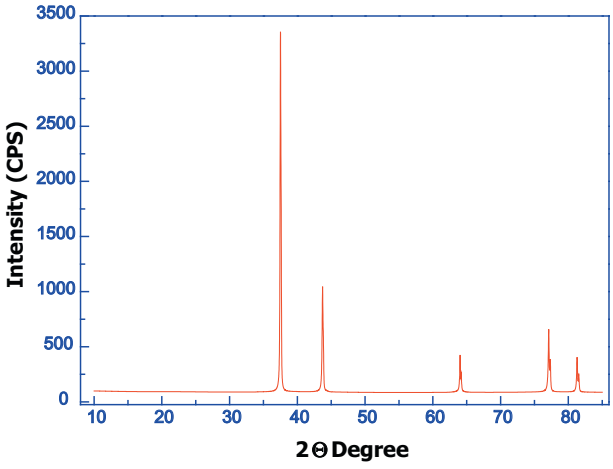

Figure 2 The XRD micrograph of silver nanoparticles.

correspond to pure silver metal with face centered cubic symmetry. This result agrees with the findings of Nanda et al., 2015 who used the XRD analysis to determine the crystalline and metallic nature of Ag NPs synthesized from *P. citrinum*.

Table 3 Average grain size (D), dislocation density (δ), and strain (ε).

Particle size D nm	δ nm^{-2}	ε
54.2	3.40×10^{-4}	6.39×10^{-4}

Table 1 shows the observed and calculated lattice parameters, cell volume, space group, and differences between them according to the PDf File No. 040783. The observed and calculated crystallographic data as well as the Miller indices (hkl) are shown in Table 2, where d-spacing is the interplanar spacing, and 2θ is the diffraction angle. The Average grain size (D), dislocation density (δ) and strain (ε) for nano particles were calculated using the following equations:

$$D = 0.9\lambda/\beta\cos\theta \quad (1)$$

$$\delta = 1/D^2 \quad (2)$$

$$\varepsilon = \beta\cos\theta/4 \quad (3)$$

where β is the full–width at half–maximum of peaks and λ is the X-ray wavelength.

The mean grain size, dislocation density, and strain are given in Table 3. The average size of biosynthesized Ag NPs was 54.2 nm in size. Ag NPs stability and conductivity were good and the Ag NPs surface charge is negative (Sadowski et al., 2008).

3.2.2. EDS analysis

Measurement of EDS is illustrated in the Fig. 3 showing the formation of pure Ag NPs. However, the mass present is about 58% from all samples. EDS profile also showed a strong silver signal along with weak carbon peaks, which may be due to the carbon tape utilized for the analysis. The intense signal at 3 KeV strongly suggested that Ag was the major element, which showed an optical absorption in this range. This finding could be attributed to changes in electron density at the surface due to collective excitation of electron that called surface plasmon resonance (Khan et al., 2013). However, EDS spectrum revealed a clear identification of the elemental composition profile of the synthesized Ag NPs.

Table 1 The calculated lattice parameters, unit cell volume, and space group.

	a	b	c	α	β	γ	Volume	Space group
PDF	4.086	4.086	4.086	90	90	90	68.23	*Fm*3*m*
Silver	4.107	4.107	4.107	90	90	90	69.277	*Fm*3*m*

Table 2 The calculated, observed crystallographic data and the Miller indices.

h	k	l	2θ Calc.	2θ Abs.	Difference	d. Abs.	d. Calc.
1	1	1	37.5000	37.9469	−0.4469	2.3984	2.3712
2	0	0	43.7200	44.1015	−0.3815	2.0706	2.0535
2	2	0	64.0400	64.1373	−0.0973	1.4540	1.4521
3	1	1	77.1200	77.0091	0.1109	1.2368	1.2383
2	2	2	81.3200	81.1224	0.1976	1.1832	1.1856

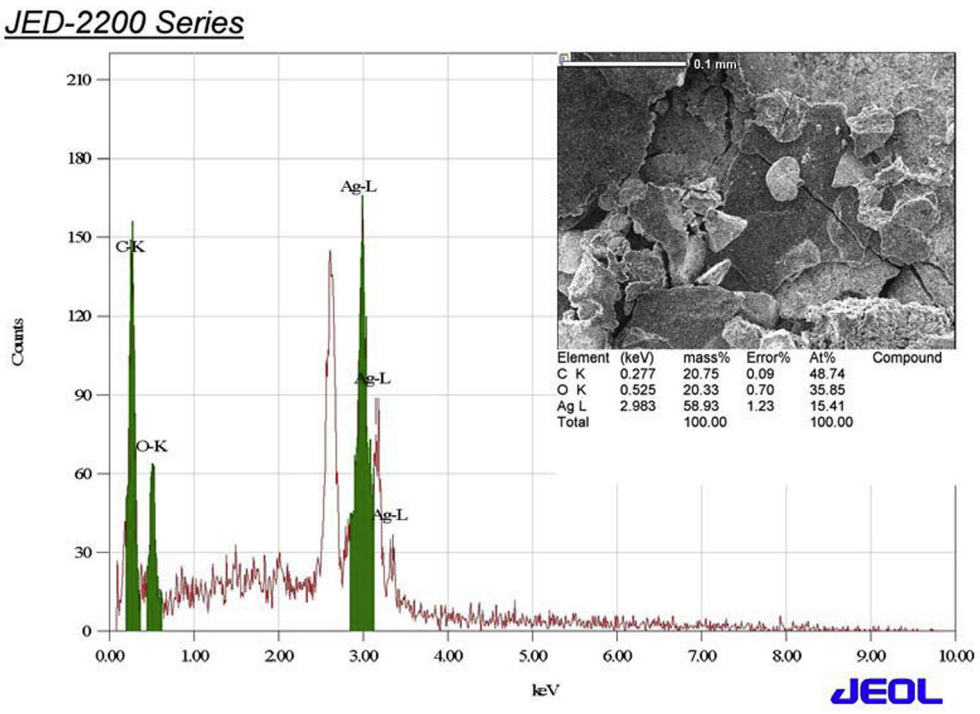

Figure 3 The EDS micrograph of biosynthesized silver nanoparticles.

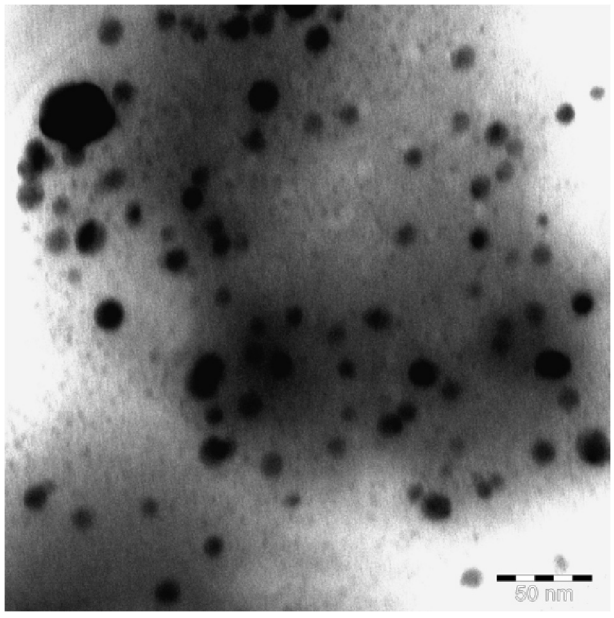

Figure 4 The TEM micrograph of biosynthesized Ag Np.

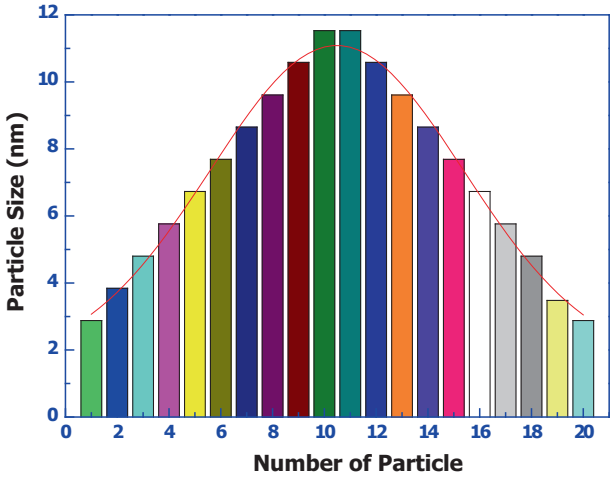

Figure 5 Gaussian distribution of biosynthesized Ag Np.

3.2.3. TEM assay

Fig. 4 illustrates the TEM micrograph of the biosynthesized Ag NPs. The particle size is clearly varied from 3 to 13 nm as well as good Gaussian variation is also obtained (Fig. 5). Ag NPs showed variable shape, and are mostly present in spherical nature. Kathiresan et al. (2009) reported that TEM micrograph of Ag NPs synthesized from *P. fellutanum* showed particle size that ranged from 5 to 25 nm. Ag NPs were generally aggregated and some of them were scattered and varying in size. Goswami et al. (2013) reported Ag NPs with sizes of 20–30 nm from *P. citrinum*.

3.2.4. Optical absorption

UV–Visible NIR Spectroscopy was used to analyze the biosynthesized Ag NPs. This technique uses the light in the visible, near ultra-violet and near infrared regions to cause electronic transitions in the target material. A light source of a fixed wavelength is shone through the sample and its absorption intensity measured against a background using a detector. The wavelength is then varied slightly using perhaps a diffractometer, and the process repeated until the absorption ratio for a spectrum of wavelengths is obtained. Fig. 6 illustrates the

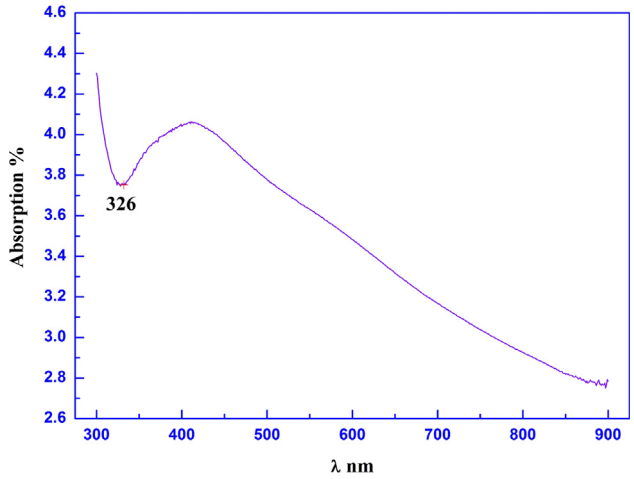

Figure 6 Optical absorption of biosynthesized silver nanoparticles.

optical absorption of biosynthesized Ag NPs and the wavelength peak clearly at 326 nm. The particle size (r) is about 1.637 nm as it is calculated from absorption peak data using Eq. (4).

$$r(nm) = \frac{-0.3049 + \sqrt{-26.23012 + \frac{10240.72}{\lambda_p(nm)}}}{-6.3829 + \frac{2483.2}{\lambda_p(nm)}} \quad (4)$$

The maximum absorbance of Ag NPs solution and the strong absorbance peak shown at 420 nm confirming the presence of Ag NPs (Nanda et al., 2015). This finding could be attributed to changes in electron density at the surface of silver due to collective excitation of electron (Elgorban et al., 2015). Honary et al. 2013 and Goswami et al., 2013 also demonstrated that UV–Vis spectrum of Ag NPs produced by *P. citrinum* exhibited an absorption band at around 400–420 nm, suggesting the synthesis of Ag NPs by this fungus. There are a number of factors that contribute to scattering intensity including the scattering angle, the refractive index of the particle, and the distance to the particle. However, in this method, only the two factors of particle size and the wavelength of incident light will be taken into account (Shivaraj et al., 2014).

3.3. Antifungal activity

Biosynthesized Ag NPs using *P. citrinum* in this study were successfully suppressed the *in vitro* growth of aflatoxigenic *A. flavus var. columnaris*. The fungal growth was generally decreased with the increase of the Ag NPs concentration. Fig. 7 illustrates the growth of *A. flavus var. columnaris* in the PDA amended with Ag NPs. The efficacy of Ag NPs ranged from 20.28 to 50.00% and the estimated ED50 and ED95 by linear regression were 224.5 ppm and 4001.8 ppm respectively (Table 4). These results confirm the findings of several researchers who demonstrated that Ag NPs had a significant effect on plant pathogenic *Rhizoctonia solani*, *Fusarium solani*, *Alternaria alternata*, *A. flavus*, *A. ochraceus* and *Aspergillus Parasiticus* (Abdel-Hadi et al., 2014; Elgorban et al., 2015; Mousavi and Pourtalebi, 2015). Antimicrobial activity of Ag NPs had frequently been attributed to the alteration of cell wall and cytoplasm as well as membrane permeability (Manjumeena et al., 2014). It was also reported that fungal DNA loses its ability to duplicate following Ag^+ treatment, as well as the synthesis of enzymes and cellular proteins, and adenine triphosphate (ATPs) could also be affected (Feng et al., 2000; Sang et al., 2012; Elgorban et al., 2015).

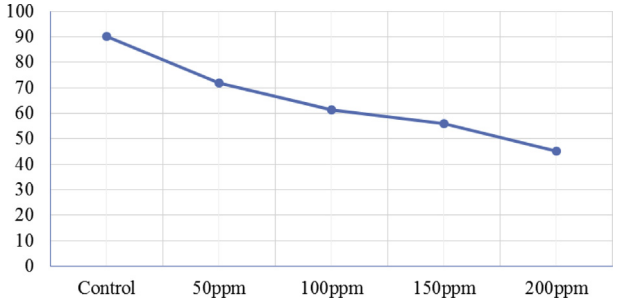

Figure 7 The growth of *Aspergillus flavus var. columnaris* in the PDA amended with different doses of biosynthesized Ag NPs.

Table 4 Efficacy (%) of biosynthesized Ag NPs on *A. flavus var. columnaris*.

50 ppm	100 ppm	150 ppm	200 ppm	ED_{50}	ED_{95}	Slope ± SE
20.28	31.94	37.78	50.00	224.5	4001.8	1.31 ± 8.09

ED_{50} = median effective dose.
ED_{95} = the dose required foe desired effect in 95% of the population exposed to it.
SE = the standard error.

The grape molding fungus *P. citrinum* in the present study has a capability of synthesize Ag NPs. The obtained Ag NPs were successfully inhibited by the *in vitro* growth of aflatoxigenic isolate of *A. flavus var. columnaris*. Further work is needed to confirm this efficacy against other mycotoxigenic strains and to determine the potent applicable doses.

Acknowledgment

The authors would like to extend their sincere appreciation to the Deanship of Scientific Research at King Saud University for its funding this Research group No (RG-1436-09).

References

Abdel-Hadi, A.M., Awad, M.F., Abo-Dahab, N.F., ElKady, M.F., 2014. Extracellular synthesis of silver nanoparticles by *Aspergillus terreus*: biosynthesis, characterization and biological activity. Biosci. Biotechnol. Res. Asia 11 (3), 1179–1186.

Arapcheska, M., Jovanovska, V., Jankuloski, Z., Musliu, Z.H., Uzunov, R., 2015. Impact of aflatoxins on animal and human health. Int. J. Innov. Sci. Eng. Technol. 2 (2), 156–161.

Carvajal, R.J.R., 1993. advances in magnetic structure determination by neutron powder diffraction. Phys. B 192, 55–69.

Devi, T.P., Kulanthaivel, S., Kamil, D., Borah, J.L., Prabhakaran, N., Srinivasa, N., 2013. Biosynthesis of silver nanoparticles from *Trichoderma* species. Indian J. Exp. Biol. 51 (7), 543–547.

Elgorban, A.M., El-Samawaty, A.M., Yassin, M.A., Sayed, S.R., Adil, S.F., Elhindi, K.M.M., Bakri, M., Khan, M., 2015. Antifungal

silver nanoparticles: synthesis, characterization and biological evaluation. Biotechnol. Biotechnol. Equip. 30 (1), 56–62.
Feng, Q.L., Wu, J., Chen, G.Q., Cui, F.Z., Kim, T.N., Kim, J.O., 2000. A mechanistic study of the antibacterial effect of silver ions on *Escherichia coli* and *Staphylococcus aureus*. J. Biomed. Mater. Res. 52, 662–668.
Gade, A., Gaikwad, S., Duran, N., Rai, M., 2014. Green synthesis of silver nanoparticles by *Phoma glomerata*. Micron 59, 52–59.
Gajbhiye, M., Kesharwani, J., Ingle, A., Gade, A., Rai, M., 2009. Fungus mediated synthesis of silver nanoparticles and their activity against pathogenic fungi in combination with fluconazole. Nanomed. Nanotechnol. Biol. Med. 5 (4), 382–386.
Ghorbani, H.R., Safekordi, A.A., Attar, H., Rezayat Sorkhabadi, S. M., 2011. Biological and non-biological methods for silver nanoparticles synthesis. Chem. Biochem. Eng. Q. 25, 317–326.
Goswami, A.M., Sarkar, T.S., Ghosh, S., 2013. An Ecofriendly synthesis of silver nano-bioconjugates by *Penicillium citrinum* (MTCC9999) and its antimicrobial effect. AMB Express 3, 16. http://dx.doi.org/10.1186/2191-0855-3-16.
Honary, S., Barabadi, H., Gharaei-Fathabad, E., Naghibi, F., 2013. Green synthesis of silver nanoparticles induced by the fungus *Penicillium citrinum*. Trop. J. Pharm. Res. 12, 7–11.
Ingle, A., Gade, A., Bawaskar, M., Rai, M., 2009. *F. solani*: a novel biological agent for the extracellular synthesis of silver nanoparticles. J. Nanopart. Res. 11 (8), 2079–2085.
Kathiresan, K., Manivannan, S., Nabeel, A.M., Dhivya, B., 2009. Studies on silver nanoparticles synthesized by a marine fungus *Penicillium fellutanum* isolated from coastal mangrove sediment. Colloids Surf. B 71 (1), 133–137.
Khalil, N.M., 2013. Biogenic silver nanoparticles by *Aspergillus terreus* as a powerful nanoweapon against *Aspergillus fumigatus*. Afr. J. Microbiol. Res. 7 (50), 5645–5651.
Khan, M., Adil, S.F., Tahir, M.N., Tremel, W., Alkhathlan, H.Z., Warthan, A., Siddiqui, M.R.H., 2013. Green synthesis of silver nanoparticles mediated by *Pulicaria glutinosa* extract. Int. J. Nanomed. 8, 1507–1516.
Manjumeena, R., Duraibabu, D., Sudha, J., Kalaichelvan, P.T., 2014. Biogenic nanosilver incorporated reverse osmosis membrane for antibacterial and antifungal activities against selected pathogenic strains: an enhanced eco-friendly water disinfection approach. J. Environ. Sci. Health, Part A: Toxic/Hazard. Subst. Environ. Eng. 49, 1125–1133.
Mousavi, S.A.A., Pourtalebi, S., 2015. Inhibitory effects of silver nanoparticles on growth and aflatoxin B1 production by *Aspergillus Parasiticus*. Iran. J. Med. Sci. 40 (6), 501–506.
Nanda, A., Majeed, S., Abdullah, M.S., Nayak, B.K., Rizvi, E.H., 2015. Efficacy of nanosilver from soil fungus enhancing the antiseptic activity of Ciprofloxacin against pathogenic bacteria. Der. Pharma Chem. 7 (6), 141–146.
Naveen, H.K.S., Kumar, G., Karthik, L., Rao, B.K.V., 2010. Extracellular biosynthesis of silver nanoparticles using filamentous fungus *Penicillium* sp. Arch. Appl. Sci. Res. 2 (6), 161–167.
Prema, P., 2010. Chemical mediated synthesis of silver nanoparticles and its potential antibacterial application. Anal. Model. Technol. Appl., 151–166
Sadowski, Z., Maliszewska, I.H., Grochowalska, B., Polowczyk, I., Kozlecki, T., 2008. Synthesis of silver nanoparticles using microorganisms. Mater. Sci. Pol. 26 (2), 419–424.
Sang, W.K., Jin, H.J., Kabir, L., Yun, S.K., Ji, S.M., Youn, S.L., 2012. Antifungal effects of silver nanoparticles (Ag NPs) against various plant pathogenic fungi. Mycobiology 40, 415–427.
Saxena, J., Sharma, M.M., Gupta, S., Singh, A., 2014. Emerging role OF Fungi IN nanoparticle synthesis and their applications. World J. Pharm. Pharm. Sci. 3 (9), 1586–1613.
Shivaraj, N., Vandana, R., Dattu, S., 2014. Characterization and biosynthesis of silver nanoparticles using a fungus *Aspergillus niger*. Int. Lett. Nat. Sci. 15, 49–57.
Singh, D., Rathod, V., Ninganagouda, S., Hiremath, J., Singh, A.K., Mathew, J., 2014. Optimization and characterization of silver nanoparticle by endophytic fungi *Penicillium* sp. isolated from *Curcuma longa* (Turmeric) and application studies against MDR *E. coli* and *S. aureus*. Bioinorg. Chem. Appl., 405021
Thul, S.T., Sarangi, B.K., Panday, R.A., 2013. Nanotechnology in agro-ecosystem: implications on plant productivity and its soil environment. Expert Opin. Environ. Biol. 2, 1. http://dx.doi.org/10.4172/2325-9655.1000101.
Yassin, M.A., Moslem, M.A., El-Samawaty, A.M.A., El-Shikh, M.S., 2013. Effectiveness of *Allium sativum* in controlling sorghum grain molding fungi. J. Pure Appl. Microbiol. 7 (1), 101–107.